Editors' Suggestion

Parity Transition of Spin-Singlet Superconductivity Using Sublattice Degrees of Freedom

Shiki Ogata,[1] Shunsaku Kitagawa,[1,*] Katsuki Kinjo,[1] Kenji Ishida,[1] Manuel Brando,[2] Elena Hassinger,[3] Christoph Geibel,[2] and Seunghyun Khim[2]
[1]Department of Physics, Kyoto University, Kyoto 606-8502, Japan
[2]Max Planck Institute for Chemical Physics of Solids, D-01187 Dresden, Germany
[3]Technical University Dresden, Institute for Solid State and Materials Physics, 01062 Dresden, Germany

(Received 15 December 2022; accepted 24 March 2023; published 19 April 2023)

Recently, a superconducting (SC) transition from low-field (LF) to high-field (HF) SC states was reported in $CeRh_2As_2$, indicating the existence of multiple SC states. It has been theoretically noted that the existence of two Ce sites in the unit cell, the so-called sublattice degrees of freedom owing to the local inversion symmetry breaking at the Ce sites, can lead to the appearance of multiple SC phases even under an interaction inducing spin-singlet superconductivity. $CeRh_2As_2$ is considered as the first example of multiple SC phases owing to this sublattice degree of freedom. However, microscopic information about the SC states has not yet been reported. In this study, we measured the SC spin susceptibility at two crystallographically inequivalent As sites using nuclear magnetic resonance for various magnetic fields. Our experimental results strongly indicate a spin-singlet state in both SC phases. In addition, the antiferromagnetic phase, which appears within the SC phase, only coexists with the LF SC phase; there is no sign of magnetic ordering in the HF SC phase. The present Letter reveals unique SC properties originating from the locally noncentrosymmetric characteristics.

DOI: 10.1103/PhysRevLett.130.166001

In conventional superconductors, a superconducting (SC) order parameter can be classified as the multiplication of spin and orbital states, that is, even-parity spin-singlet and odd-parity spin-triplet states. One possible expansion of the framework in SC symmetry is to introduce additional degrees of freedom, such as frequency and atomic orbital state [1,2]. As shown in Fig. 1(a), in a two-dimensional system with locally broken inversion symmetry (centrosymmetric, but no inversion center at the SC layers), there are sublattice degrees of freedom owing to the inversion symmetry operation between the two layers. In such systems, a parity transition from a low-field (LF) even-parity SC state to a high-field (HF) odd-parity pair-density-wave (PDW) SC state (the SC phase is inverted layer by layer) [Fig. 1(b)] is theoretically proposed, even when only a pairing interaction in the spin-singlet channel exists [3]. The PDW state coexisting with the charge-density-wave state has been discussed in high-SC transition temperature T_{SC} cuprates [4] and kagome superconductors [5]; however, the PDW phase originating from crystal symmetry is quite rare.

$CeRh_2As_2$, where the local inversion symmetry is broken at the Ce sites, is a recently discovered superconductor with $T_{SC} \sim 0.3$ K [6]. In $CeRh_2As_2$, a SC transition from the SC1 to SC2 phase occurring at approximately 4 T was reported for $H \| c$. This is the first

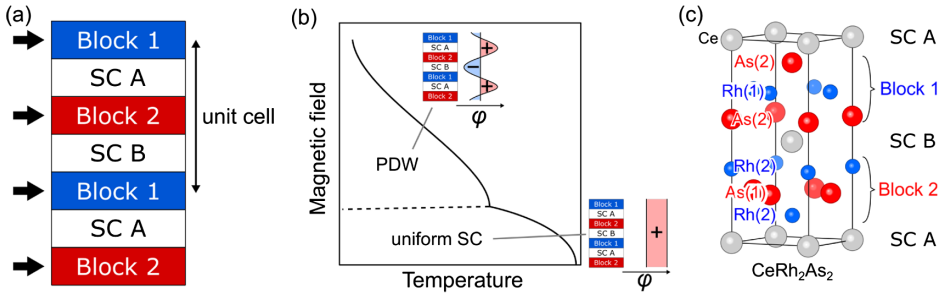

FIG. 1. Schematics of a PDW state in a two-dimensional system with locally broken inversion symmetry. (a) Schematic image of crystal structure. The unit cell contains two kinds of superconducting layers. The position of the inversion center is indicated by the arrows. (b) Theoretically predicted H–T phase diagram. The position dependence of superconducting order parameters in each superconducting phase is shown by the schematic images. (c) Crystal structure of $CeRh_2As_2$.

experimental indication of the SC parity transition originating from the sublattice degrees of freedom and has promoted many theoretical studies [7–13]. However, to date, there have been few experimental investigations on the SC properties [14–16]. Therefore, further experimental confirmation is required.

The crystal structure of $CeRh_2As_2$ is of the tetragonal $CaBe_2Ge_2$ type with space group $P4/nmm$ (No. 129, D_{4h}^7) [17]. There are two crystallographically inequivalent As and Rh sites. As(1) [Rh(1)] is tetrahedrally coordinated by Rh(2) [As(2)], as shown in Fig. 1(c). Heavy-fermion superconductivity is characterized by a broad maximum in resistivity at $T_{coh} \sim 40$ K and a large specific heat jump at T_{SC} [6]. In addition to the multiple SC phases, $CeRh_2As_2$ exhibits nonmagnetic and magnetic phase transitions just above and below T_{SC}, respectively [6,14]. The specific heat shows a large anomaly at T_{SC} and a rather weak anomaly at $T_0 \sim 0.4$ K. The anomaly at T_0 is considered as a phase transition to an electric quadrupole density-wave state [18]. Moreover, nuclear quadrupole resonance (NQR) measurements revealed an antiferromagnetic (AFM) order inside the SC phase [14]. Hence, $CeRh_2As_2$ is a promising system for studying the role of sublattice degrees of freedom for unconventional nonmagnetic, AFM, and SC states, as well as their interactions.

Nuclear magnetic resonance (NMR) can measure spin susceptibility in the SC state, whereas bulk magnetic susceptibility is dominated by a SC diamagnetic shielding effect. In addition, NMR is sensitive to the appearance of internal magnetic fields at observed nuclear sites. Therefore, NMR is one of the most powerful techniques for studying SC and magnetic properties. Furthermore, NMR is also useful for detecting spatially modulated SC states, such as the Fulde-Ferrell-Larkin-Ovchinnikov and PDW phases, because NMR measures the local spin susceptibility at the nuclear positions [19].

In this Letter, we report the ^{75}As-NMR results for $CeRh_2As_2$. Up to 5 T, the spin susceptibility decreased in the SC state, indicating spin-singlet superconductivity in both the SC1 and SC2 phases. The decrease in the Knight shift in the SC1 phase was in good agreement with the critical field of the SC1–SC2 transition. In contrast, the decrease in the Knight shift in the SC2 phase is seemingly inconsistent with the large H_{c2}, suggesting the spatial modulation of the SC spin susceptibility. This is the first microscopic information on the unique SC states in $CeRh_2As_2$.

Single crystals of $CeRh_2As_2$ were grown using the bismuth flux method [6]. The magnetic field dependence of T_{SC} and the temperature dependence of the critical field of the SC1–SC2 transition were determined from the ac susceptibility measurements using a NMR coil as shown in the Supplemental Material [20]. The details in NMR measurements are also described in the Supplemental Material [20]. We experimentally confirmed the superconductivity immediately after the NMR pulses using a technique reported in a previous study [21,22]. Reflecting two crystallographically inequivalent As sites, two NMR peaks were observed in all measurement ranges, as shown in Figs. 2(a) and 2(e). The site

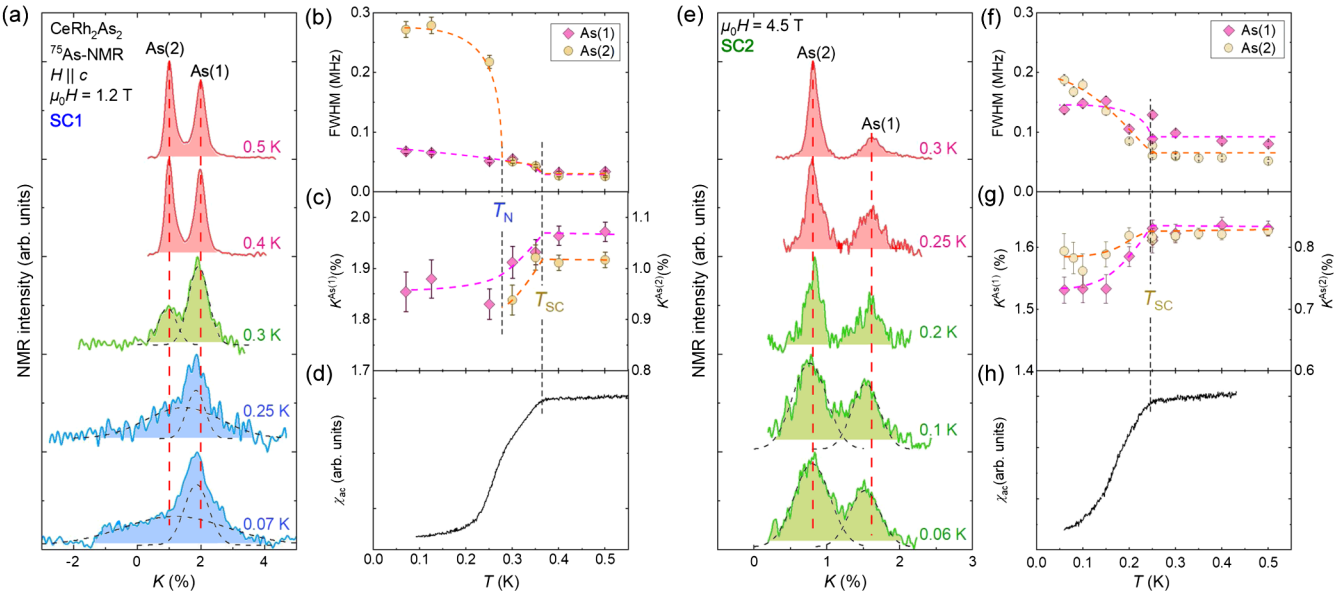

FIG. 2. NMR measurements in $CeRh_2As_2$. (a) NMR spectra at 1.2 T for $H\|c$ measured at various temperatures. The dashed curves indicate the results of a two-peak fitting. (b) Temperature dependence of full width at half maximum (FWHM), (c) Knight shift at the As(1) site $K^{As(1)}$ and As(2) site $K^{As(2)}$, determined by NMR spectrum at 1.2 T. T_{SC} and T_N are indicated by the dashed lines. The dashed curves are guides for the eye. (d) Temperature dependence of ac magnetic susceptibility at 1.2 T for $H\|c$. (e) NMR spectra at 4.5 T for $H\|c$ measured at various temperatures. (f) Temperature dependence of FWHM, (g) Knight shift, (h) and ac magnetic susceptibility at 4.5 T for $H\|c$.

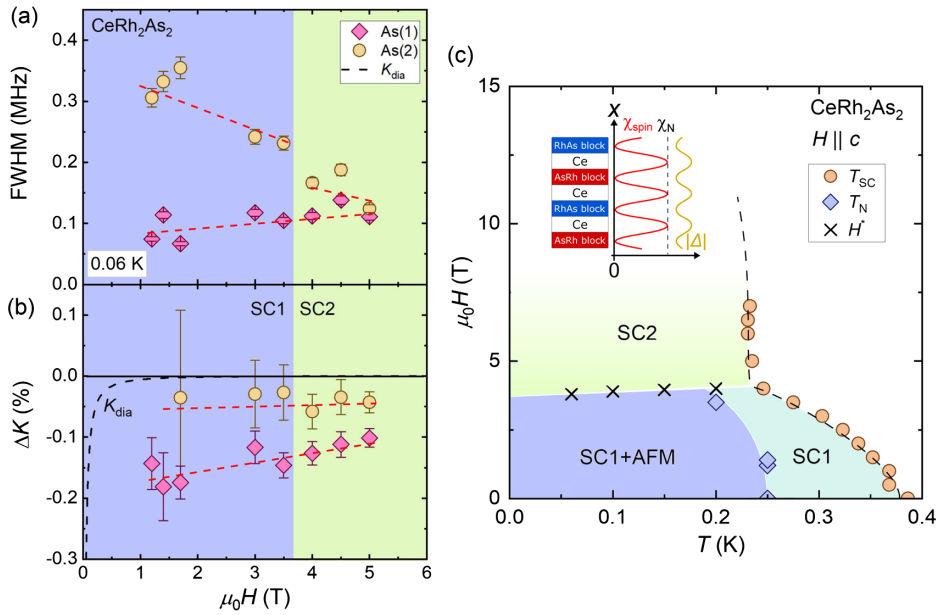

FIG. 3. Magnetic field variation of the magnetic properties in $CeRh_2As_2$. The c-axis magnetic field dependence of FWHM at (a) 0.06 K and (b) $\Delta K = K(0.06\ \mathrm{K}) – K(0.6\ \mathrm{K})$. The dashed curve indicates the contribution of SC diamagnetism K_{dia}. The dashed lines are guides for the eye. (c) The H–T phase diagram in the present sample of $CeRh_2As_2$ determined from the NMR and ac magnetic susceptibility measurements. Circles denote T_{SC} determined by the onset temperature of the SC diamagnetic signal from ac magnetic susceptibility. Crosses denote the critical magnetic field of the SC1–SC2 transition determined by the anomaly of ac magnetic susceptibility. Diamonds indicate T_N determined by the increase in NMR linewidth. Inset: schematic image of the distribution of spin susceptibility and SC gap.

assignment of two NMR peaks has been described in a previous paper [23]. The reason why the NMR spectrum of the As(1) site is broad at 4.5 T is a slight misalignment of the magnetic field direction from the c axis ($< 2°$ in this experiment).

First, we show the temperature evolution of the NMR spectrum for each SC phase. As shown in Fig. 2(a), at 1.2 T (low-field SC1 phase), two sharp peaks were observed above $T_{\mathrm{SC}} \sim 0.35$ K. Below T_{SC}, the NMR spectrum broadens, owing to the SC diamagnetic field, and significant site-dependent broadening is observed below 0.25 K. The site-dependent broadening was also observed at zero field (NQR measurements) [14], which was attributed to the AFM order. The internal field at the As(2) site is estimated to be ~20 mT. In contrast, at 4.5 T in the SC2 phase, the NMR lines broaden just below T_{SC} for both sites, as in the SC1 phase, but there is no additional site-dependent broadening at lower temperatures, down to 0.06 K. This indicates the absence of AFM ordering below T_{SC} in the SC2 phase. To investigate the spin susceptibility at the two As sites, NMR Knight shifts are determined by two-peak Gaussian fitting. The Knight shifts for the As(1) and As(2) sites are denoted by $K^{\mathrm{As(1)}}$ and $K^{\mathrm{As(2)}}$, respectively. $K^{\mathrm{As(1)}}$ decreases below T_{SC} in both SC phases. In the SC2 phase, $K^{\mathrm{As(2)}}$ also decreases, while in the SC1 phase $K^{\mathrm{As(2)}}$ is not measurable owing to the extremely broad spectrum below the AFM transition temperature T_N.

To clarify the magnetic field evolution of the spin susceptibility and the AFM order, the magnetic field dependence of the FWHM at the lowest temperature (0.06 K) and $\Delta K = K(0.06\ \mathrm{K}) – K(0.6\ \mathrm{K})$ are shown in Figs. 3(a) and 3(b), respectively. In the SC1 phase, the linewidth of the As(2) site decreases as the magnetic field increases, but remains significantly broader than that of As(1) until 3.5 T. Between 3.5 and 4 T, the width of the As(2) lines drops to values only slightly higher than that of As(1). In contrast, in the SC2 phase, the linewidth of the As(2) site is almost the same as that of the As(1) site. The absence of an internal field at the As(2) site indicates that the AFM phase only coexists with the SC1 phase, not with the SC2 phase. In contrast to the magnetic field dependence of the linewidth, $|\Delta K|$ at both As sites does not show any anomaly at the phase boundary and gradually decreases as the magnetic field increases, up to 5 T. The magnetic field dependence of $|\Delta K^{\mathrm{As(1)}}|$ can be extrapolated to zero at 14 T (H_{c2}), suggesting that the magnetic field dependence of $|\Delta K|$ originates from the field-induced quasiparticle density of states (Volovik effect). $|\Delta K^{\mathrm{As(2)}}|$ is smaller than $|\Delta K^{\mathrm{As(1)}}|$ owing to the difference of the hyperfine coupling constant A_{hf} [23].

From the ac magnetic susceptibility and NMR measurements, we constructed the H–T phase diagram in the present sample of $CeRh_2As_2$, as shown in Fig. 3(c). The previously reported peculiar shape of T_{SC} and the SC1–SC2 transition were reproduced by our measurements,

whereas $T_{SC} = 0.37$ K was higher than that of the previous samples [6,16]. This is due to the differences in sample quality and experimental methods. Our NMR results indicate that the AFM phase disappears in the SC2 phase, which is strong evidence of the presence of the SC1–SC2 transition and the different SC properties between the two phases. Furthermore, the smooth connection of the Knight shift between two SC states indicates that the SC2 state is a nonpolarized one. This is in complete contrast to the usual field-induced destruction of an AFM state resulting in a polarized ferromagneticlike state. Therefore, the observed field-induced transition from an AFM state to a state with no sizable polarization at high field is a highly unusual one, indicating that this AFM state is strongly linked to the SC1 state.

The SC spin state can be deduced from the temperature variation in the NMR Knight shift. In a conventional spin-singlet superconductor, the spin component of the Knight shift decreases in the SC state and becomes almost zero at $T \to 0$ K. However, when the SC spins of spin-triplet superconductors are aligned along the magnetic field, the spin component of the Knight shift does not change across T_{SC}. As the Knight shift includes various contributions, such as the temperature-independent orbital component arising from the Van Vleck susceptibility and SC diamagnetic effect, the absolute amount of the spin component of the Knight shift must be evaluated. K at the lowest temperature can be divided into the following three contributions:

$$K = K_{\text{normal}} + \delta K_{\text{spin}} + K_{\text{dia}}, \tag{1}$$

where K_{normal} is the normal-state Knight shift, δK_{spin} is the change in a spin component of the Knight shift in the SC state, and K_{dia} is the SC diamagnetic component. In the SC state, the Knight shift decreases owing to the SC diamagnetic shielding effect, and the value of K_{dia} at 0 K is approximately expressed as [24]

$$K_{\text{dia}} = -\frac{H_{c1}}{H}\frac{\ln(\frac{\beta\lambda_d}{\sqrt{e}\xi})}{\ln\kappa}. \tag{2}$$

Here, H_{c1} is the SC lower critical field, ξ is the Ginzburg-Landau (GL) coherence length, and β is a factor that depends on the vortex structure and is 0.38 for the triangular vortex lattice. λ_d is the distance between the vortices and is calculated using the relation $\phi_0 = (\sqrt{3}/2)\lambda_d^2(\mu_0 H_{\text{ext}})$, e is Euler's number, and κ is the GL parameter. From the SC upper critical field $\mu_0 H_{c2} = 14$ T and thermodynamic critical field $\mu_0 H_c = 31$ mT [6], $\mu_0 H_{c1} = 0.40$ mT, $\xi = 4.85$ nm, and $\kappa = 319$ were obtained. As shown in Fig. 3(b), the magnetic field dependence of K_{dia} is negligibly small compared to the experimental δK. In addition, the temperature dependence of K_{normal} shows almost constant at low temperatures [23], as shown in Figs. 2(c) and 2(g). Therefore, ΔK was dominated by δK_{spin}. As shown in Figs. 2(c) and 2(g), a clear decrease in K was observed in the SC state, indicating the realization of spin-singlet superconductivity in both the SC1 and SC2 phases.

The spin-singlet superconductivity in the SC1 phase can also be confirmed by the quantitative agreement between H_{c2} and the Pauli limiting field H_P estimated from the reduction in the Knight shift. In strongly correlated electron systems, spin-singlet superconductivity is destroyed when the Zeeman-splitting energy is as high as the SC condensation energy, called the Pauli limiting effect. It is well known that in a spin-singlet superconductor, a relation holds between H_P and the decrease in the spin susceptibility $\delta\chi$ ascribed to singlet-pair formation. This is expressed as

$$\frac{1}{2}\delta\chi\mu_0 H_P(0)^2 = \frac{1}{2}\mu_0 H_c^2. \tag{3}$$

This equation yields $\mu_0 H_P(0) = \mu_0 H_c/\sqrt{|\delta\chi|}$, where $\delta\chi$ can be determined from ΔK as $\delta\chi = (\mu_B N_A/A_{\text{hf}})\Delta K$. In the SC1 phase, ΔK at the As(1) site is approximately -0.2%; thus, $\mu_0 H_P(0)$ is estimated to be 3.4 T with $\mu_0 H_c = 31$ mT and the hyperfine coupling constant $A_{\text{hf}}^{\text{As(1)}} = 1.55$ T$/\mu_B$ [23]. The estimated $\mu_0 H_P(0)$ agrees with the SC1–SC2 transition field ($\sim$4 T), indicating that the SC1 phase exhibits homogeneous spin-singlet superconductivity. Such a correspondence between the critical field and ΔK is observed in various spin-singlet heavy-fermion superconductors [25–28].

In contrast, ΔK in the SC2 phase is unusual. K in the SC2 phase also clearly decreases, and $\mu_0 H_P(0)$ is estimated to be 4.8 T from $\Delta K^{\text{As(1)}} = -0.1\%$, which is much smaller than $\mu_0 H_{c2}(0) = 14$ T. Here, we assume the same H_c as in the SC1 state. If we consider that $H_P(0)$ increases owing to an increase in H_c in the SC2 phase, the H_c should be increased by a factor of 3, which is an unrealistic value in this case. It is noteworthy that $\Delta K^{\text{As(2)}} = -0.05\%$ and $A_{\text{hf}}^{\text{As(2)}} = 0.27$ T$/\mu_B$ also lead to a small Pauli limiting field, $\mu_0 H_P(0) = 2.8$ T. There are several superconductors without the Pauli limiting effect owing to the absence of the spin susceptibility reduction [29–31], but the case where the Pauli limiting effect does not work despite a decrease in the spin susceptibility is quite rare. The discrepancy between the decrease in the spin susceptibility and the absence of the Pauli limiting field can be reconciled by the presence of a spatially inhomogeneous SC state.

Recently, SC states realized in the presence of sublattice degrees of freedom have been intensively studied, and spin susceptibility has been calculated in various SC states [32]. The average spin susceptibility in the PDW state is suggested to be the same as that in the normal state. The present Knight-shift results are inconsistent with these theoretical suggestions. To interpret this discrepancy, we propose a position-dependent modulation of spin

susceptibility in the PDW state. In this SC state, the SC order parameter oscillates along the c axis with a period corresponding to the c lattice parameter; thus, the spin susceptibility also oscillates with the same periodicity. The NMR Knight shift probes the local spin susceptibility at the observed nuclear site. Therefore, the present results imply that the block layers become the "spin-singlet" dominant SC state and the spin susceptibility at the block layers decreases in the SC2 states, as shown in the inset of Fig. 3(c). In contrast, a sizable Rashba effect at the Ce site would lead to locally spin-polarized bands. The Pauli susceptibility would then transform into a Van Vleck susceptibility, which is insensitive to superconductivity [32,33]. As a result, the spin susceptibility in the SC state at the Ce sites would be of similar size as that in the normal state.

In $CeRh_2As_2$, the SC properties are determined by the Ce layer, resulting in the spin susceptibility of the Ce layers being crucially modified by the SC character. We suggest the possibility that the spin susceptibility at the Ce layers largely changes between the LF and HF SC states; that is, the spin susceptibility at the Ce site decreases in the SC1 state but remains unchanged in the SC2 state, although the spin susceptibility at the block layers does not change significantly. This might explain the large difference in the Pauli limiting field between the two phases. However, because all NMR-active Ce isotopes are unstable, measuring the spin susceptibility at the Ce site is impossible. Thus, we need to seek other methods to determine the spatial modulation of the spin susceptibility in $CeRh_2As_2$. In addition, theoretical studies on spin susceptibility modulation in the PDW state are required.

In conclusion, we measured the SC spin susceptibility in the LF and HF SC states. The spin susceptibility decreases in both SC states, indicating a spin-singlet state. The discrepancy between the decrease in the spin susceptibility and the absence of the Pauli limit might be explained by the spatially modulated spin susceptibility in the SC2 state. In addition, NMR measurements revealed that the AFM phase only coexists with the LF SC phase, indicating a strong link to the SC1 state. Our findings help to understand the unique multi-SC state in $CeRh_2As_2$.

This work was partially supported by the Kyoto University LTM Center and Grants-in-Aid for Scientific Research (KAKENHI) (Grants No. JP19K14657, No. JP19H04696, No. JP20H00130, No. JP21K18600 and No. JP22H04933). C. G. and E. H. acknowledge support from the DFG program Fermi-NESt through Grant No. GE 602/4-1. Additionally, E. H. acknowledges funding by the DFG through CRC1143 (Project No. 247310070) and the Würzburg-Dresden Cluster of Excellence on Complexity and Topology in Quantum Matter—ct.qmat (EXC 2147, Project ID 390858490).

S. O. and S. K. contributed equally to this work.

*kitagawa.shunsaku.8u@kyoto-u.ac.jp

[1] J. Linder and A. V. Balatsky, Odd-frequency superconductivity, Rev. Mod. Phys. **91**, 045005 (2019).
[2] H. G. Suh, H. Menke, P. M. R. Brydon, C. Timm, A. Ramires, and D. F. Agterberg, Stabilizing even-parity chiral superconductivity in Sr_2RuO_4, Phys. Rev. Res. **2**, 032023(R) (2020).
[3] T. Yoshida, M. Sigrist, and Y. Yanase, Pair-density wave states through spin-orbit coupling in multilayer superconductors, Phys. Rev. B **86**, 134514 (2012).
[4] D. F. Agterberg, J. S. Davis, S. D. Edkins, E. Fradkin, D. J. V. Harlingen, S. A. Kivelson, P. A. Lee, L. Radzihovsky, J. M. Tranquada, and Y. Wang, The physics of pair-density waves: cuprate superconductors and beyond, Annu. Rev. Condens. Matter Phys. **11**, 231 (2020).
[5] H. Chen *et al.*, Roton pair density wave in a strong-coupling kagome superconductor, Nature (London) **599**, 222 (2021).
[6] S. Khim, J. F. Landaeta, J. Banda, N. Bannor, M. Brando, P. M. R. Brydon, D. Hafner, R. Küchler, R. Cardoso-Gil, U. Stockert, A. P. Mackenzie, D. F. Agterberg, C. Geibel, and E. Hassinger, Field-induced transition within the superconducting state of $CeRh_2As_2$, Science **373**, abe7518 (2021).
[7] E. G. Schertenleib, M. H. Fischer, and M. Sigrist, Unusual $H-T$ phase diagram of $CeRh_2As_2$: The role of staggered noncentrosymmetricity, Phys. Rev. Res. **3**, 023179 (2021).
[8] K. Nogaki, A. Daido, J. Ishizuka, and Y. Yanase, Topological crystalline superconductivity in locally noncentrosymmetric $CeRh_2As_2$, Phys. Rev. Res. **3**, L032071 (2021).
[9] A. Skurativska, M. Sigrist, and M. H. Fischer, Spin response and topology of a staggered-Rashba superconductor, Phys. Rev. Res. **3**, 033133 (2021).
[10] D. Möckli and A. Ramires, Two scenarios for superconductivity in $CeRh_2As_2$, Phys. Rev. Res. **3**, 023204 (2021).
[11] D. Möckli and A. Ramires, Superconductivity in disordered locally noncentrosymmetric materials: An application to $CeRh_2As_2$, Phys. Rev. B **104**, 134517 (2021).
[12] A. Ptok, K. J. Kapcia, P. T. Jochym, J. Łażewski, A. M. Oleś, and P. Piekarz, Electronic and dynamical properties of $CeRh_2As_2$: Role of Rh2As2 layers and expected orbital order, Phys. Rev. B **104**, L041109 (2021).
[13] D. C. Cavanagh, T. Shishidou, M. Weinert, P. M. R. Brydon, and D. F. Agterberg, Nonsymmorphic symmetry and field-driven odd-parity pairing in $CeRh_2As_2$, Phys. Rev. B **105**, L020505 (2022).
[14] M. Kibune, S. Kitagawa, K. Kinjo, S. Ogata, M. Manago, T. Taniguchi, K. Ishida, M. Brando, E. Hassinger, H. Rosner, C. Geibel, and S. Khim, Observation of Antiferromagnetic Order as Odd-Parity Multipoles inside the Superconducting Phase in $CeRh_2As_2$, Phys. Rev. Lett. **128**, 057002 (2022).
[15] S. Onishi, U. Stockert, S. Khim, J. Banda, M. Brando, and E. Hassinger, Low-Temperature Thermal Conductivity of the Two-Phase Superconductor $CeRh_2As_2$, Front. Electron. Mater **2**, 880579 (2022).
[16] J. F. Landaeta, P. Khanenko, D. C. Cavanagh, C. Geibel, S. Khim, S. Mishra, I. Sheikin, P. M. R. Brydon, D. F. Agterberg, M. Brando, and E. Hassinger, Field-Angle Dependence Reveals Odd-Parity Superconductivity in $CeRh_2As_2$, Phys. Rev. X **12**, 031001 (2022).

[17] R. Madar, P. Chadouet, J. P. Senateur, S. Zemni, and D. Tranqui, New ternary pnictides with the $CaBe_2Ge_2$-type structure in the systems, rare-earth-Rh P and rare-earth-Rh As, J. Less-Common Met. **133**, 303 (1987).

[18] D. Hafner, P. Khanenko, E.-O. Eljaouhari, R. Küchler, J. Banda, N. Bannor, T. Lühmann, J. F. Landaeta, S. Mishra, I. Sheikin, E. Hassinger, S. Khim, C. Geibel, G. Zwicknagl, and M. Brando, Possible Quadrupole Density Wave in the Superconducting Kondo Lattice $CeRh_2As_2$, Phys. Rev. X **12**, 011023 (2022).

[19] K. Kinjo, M. Manago, S. Kitagawa, Z. Q. Mao, S. Yonezawa, Y. Maeno, and K. Ishida, Superconducting spin smecticity evidencing the Fulde-Ferrell-Larkin-Ovchinnikov state in Sr_2RuO_4, Science **376**, 397 (2022).

[20] See Supplemental Material at http://link.aps.org/supplemental/10.1103/PhysRevLett.130.166001 for the results in ac susceptibility measurements and the details in measurements.

[21] K. Ishida, M. Manago, K. Kinjo, and Y. Maeno, Reduction of the ^{17}O Knight Shift in the Superconducting State and the Heat-up Effect by NMR Pulses on Sr_2RuO_4, J. Phys. Soc. Jpn. **89**, 034712 (2020).

[22] H. Fujibayashi, G. Nakamine, K. Kinjo, S. Kitagawa, K. Ishida, Y. Tokunaga, H. Sakai, S. Kambe, A. Nakamura, Y. Shimizu, Y. Homma, D. Li, F. Honda, and D. Aoki, Superconducting Order Parameter in UTe_2 Determined by Knight Shift Measurement, J. Phys. Soc. Jpn. **91**, 043705 (2022).

[23] S. Kitagawa, M. Kibune, K. Kinjo, M. Manago, T. Taniguchi, K. Ishida, M. Brando, E. Hassinger, C. Geibel, and S. Khim, Two-Dimensional XY-Type Magnetic Properties of Locally Noncentrosymmetric Superconductor $CeRh_2As_2$, J. Phys. Soc. Jpn. **91**, 043702 (2022).

[24] P. G. de Gennes, , *Superconductivity of Metals and Alloys* (Addison-Wesley, Reading, MA, 1989).

[25] H. Tou, K. Ishida, and Y. Kitaoka, Quasparticle spin susceptibility in heavy-fermion superconductors: An NMR study compared with specific heat results, J. Phys. Soc. Jpn. **74**, 1245 (2005).

[26] S. Kitagawa, R. Takaki, M. Manago, K. Ishida, and N. K. Sato, Spatially inhomogeneous superconducting state near Hc_2 in UPd_2Al_3, J. Phys. Soc. Jpn. **87**, 013701 (2017).

[27] S. Kitagawa, G. Nakamine, K. Ishida, H. S. Jeevan, C. Geibel, and F. Steglich, Evidence for the Presence of the Fulde-Ferrell-Larkin-Ovchinnikov State in $CeCu_2Si_2$ Revealed Using ^{63}Cu NMR, Phys. Rev. Lett. **121**, 157004 (2018).

[28] T. Hattori, H. Sakai, Y. Tokunaga, S. Kambe, T. D. Matsuda, and Y. Haga, Evidence for Spin Singlet Pairing with Strong Uniaxial Anisotropy in URu_2Si_2 Using Nuclear Magnetic Resonance, Phys. Rev. Lett. **120**, 027001 (2018).

[29] H. Mukuda, T. Ohara, M. Yashima, Y. Kitaoka, R. Settai, Y. Ōnuki, K. M. Itoh, and E. E. Haller, Spin Susceptibility of Noncentrosymmetric Heavy-Fermion Superconductor $CeIrSi_3$ under Pressure: ^{29}Si Knight-Shift Study on Single Crystal, Phys. Rev. Lett. **104**, 017002 (2010).

[30] M. Manago, K. Ishida, and D. Aoki, Absence of the Pauli-Paramagnetic Limit in a Superconducting U_6Co, J. Phys. Soc. Jpn. **86**, 073701 (2017).

[31] G. Nakamine, S. Kitagawa, K. Ishida, Y. Tokunaga, H. Sakai, S. Kambe, A. Nakamura, Y. Shimizu, Y. Homma, D. Li, F. Honda, and D. Aoki, Superconducting Properties of Heavy Fermion UTe_2 Revealed by ^{125}Te-nuclear Magnetic Resonance, J. Phys. Soc. Jpn. **88**, 113703 (2019).

[32] D. Maruyama, M. Sigrist, and Y. Yanase, Spin–orbit coupling in multilayer superconductors with charge imbalance, J. Phys. Soc. Jpn. **82**, 043703 (2013).

[33] D. Maruyama, M. Sigrist, and Y. Yanase, Locally Noncentrosymmetric superconductivity in multilayer systems, J. Phys. Soc. Jpn. **81**, 034702 (2012).